Journal of Catalysis **186,** 36–44 (1999)
Article ID jcat.1999.2532, available online at http://www.idealibrary.com on IDEAL®

Studies on Cu/CeO_2: A New NO Reduction Catalyst

Parthasarathi Bera,* S. T. Aruna,† K. C. Patil,† and M. S. Hegde*,[1]

*Solid State and Structural Chemistry Unit and †Department of Inorganic and Physical Chemistry, Indian Institute of Science, Bangalore 560 012, India

Received October 20, 1998; revised April 19, 1999; accepted April 20, 1999

Fine particle and large surface area Cu/CeO_2 catalysts of crystallite sizes in the range of 100–200 Å synthesized by the solution combustion method have been investigated for NO reduction. Five percent Cu/CeO_2 catalyst shows nearly 100% conversion of NO by NH_3 below 300°C, whereas pure ceria and Zr, Y, and Ca doped ceria show 85–95% NO conversion above 600°C. Similarly NO reduction by CO has been observed over 5% Cu/CeO_2 with nearly 100% conversion below 300°C. Hydrocarbon (*n*-butane) oxidation by NO to CO_2, N_2, and H_2O has also been demonstrated over this catalyst below 350°C making Cu/CeO_2 a new NO reduction catalyst in the low temperature window of 150–350°C. Kinetics of NO reduction over 5% Cu/CeO_2 have also been investigated. The rate constants are in the range of 1.4×10^4 to 2.3×10^4 $cm^3\ g^{-1}\ s^{-1}$ between 170 and 300°C. Cu/CeO_2 catalysts are characterized by X-ray diffraction, transmission electron microscopy, X-ray photoelectron spectroscopy, and electron paramagnetic resonance spectroscopy where Cu^{2+} ions are shown to be dispersed on the CeO_2 surface.

Key Words: **combustion synthesis; NO reduction; Cu/CeO_2; NH_3; CO; hydrocarbon.**

INTRODUCTION

NO is the prime constituent of NO_x which exists in flue gases from motor vehicles, power plants, and other combustion processes. NO_x is a pollutant that causes acid rain and smog in urban and industrial areas and it is also one of the factors for ozone layer depletion in the stratospheric region (1). So attention is focused on the catalytic reduction of NO with NH_3, CO, and hydrocarbons from the environmental point of view. Therefore, removal of NO_x offers a wide opportunity for research (2, 3).

Selective catalytic reduction (SCR) is an effective method for removing NO. Vanadia-based catalysts are commonly employed for SCR of NO with NH_3 (4). These catalysts are operated at 200–400°C. Recently amorphous chromia has been shown to be a highly active and selective catalyst for reduction of NO with NH_3 in the presence of excess O_2 (5). Noble metal (Pt, Pd, Ru) catalysts have been found to be active in the lower temperature window of 170 to 300°C (6–8). Replacing the expensive noble metals by oxide catalysts is an active area of research today.

Recently, transition metal ion exchanged zeolites have been developed for SCR of NO. Copper is one of the promising elements that has the ability to increase the SCR activity of NO with NH_3. Cu^{2+}-exchanged Y zeolite, mordenite, ZSM-5, and MFI-ferrisilicate have been found to be effective SCR catalysts for NO (9–12). Other transition metal ions such as Fe^{3+} in mesoporous Al-HMS, Al-MCM-41 have also shown good SCR activity for NO (13). Ceria-based catalysts (CeO_2–ZrO_2) have been studied extensively for oxygen storage capacity (OSC) and SCR of NO (14–16). However, relatively little study exists in the literature on transition metal ion doped CeO_2 toward NO reduction. Recently, CO oxidation over Cu/CeO_2 has been demonstrated by Flytzani-Stephanopoulos *et al.* (17, 18). The catalysts for fundamental studies are prepared by various conventional techniques such as impregnation, ion exchange, anchoring/grafting, spreading and wetting, hydrolysis, and homogeneous deposition–precipitation (2). Presently, there has been a new trend regarding novel chemical routes of synthesis that can lead to ultrafine, high-surface-area catalysts for heterogeneous catalysis. The solution combustion method has been found to be unique for obtaining high-surface-area fine particles. This method involves rapid heating at 350°C of an aqueous redox mixture containing stoichiometric amounts of corresponding metal nitrates and hydrazine-based fuels (19, 20). In this article we report the first study on NO reduction by NH_3, CO, and hydrocarbon over Cu/CeO_2 catalyst prepared by the solution combustion method. NO reduction over pure CeO_2 and Zr, Y, and Ca doped CeO_2 prepared by the solution combustion method has been studied to show that Cu/CeO_2 is a unique catalyst for NO reduction working in the low temperature window of 150–350°C.

EXPERIMENTAL

Preparation of Catalysts

Ceric ammonium nitrate (Leo Chem., 99%) and copper nitrate (S D Fine Chem., 99.9%) were used as the sources of

[1] To whom correspondence should be addressed. E-mail: mshegde@sscu.iisc.ernet.in. Fax: 91-80-3311310.

0021-9517/99 $30.00

cerium and copper. Oxalyldihydrazide (ODH, $C_2H_6N_4O_2$) prepared from diethyl oxalate and hydrazine hydrate was used as the fuel (21).

In a typical combustion synthesis, a Pyrex dish (300 cm^3) containing an aqueous redox mixture of stoichiometric amounts of ceric ammonium nitrate (5 g), copper nitrate (0.1419 g), and ODH (2.6444 g) in 100 cm^3 volume of H_2O was introduced into a muffle furnace preheated to 350°C. The solution boiled with foaming and frothing and ignited to burn with a flame yielding about 1.5 g voluminous oxide product within 5 min. Similarly Zr, Y, and Ca doped CeO_2 and 10% Cu/CeO_2 were prepared by this method from their respective metal nitrates and ODH fuel. These oxides were prepared in an open muffle furnace kept in a fuming cupboard. Exhaust was on during the firing. The reaction can be controlled by carrying out the combustion in an open atmosphere. By choosing proper sizes of the container and muffle furnace larger quantity of the catalysts (up to 500 g) can be prepared in a single batch. Since the oxides absorb the moisture, it is necessary to store them in a vacuum desiccator and heat them at 300°C for 12 h before using.

Characterization of Catalysts

The X-ray diffraction (XRD) patterns of Cu/CeO_2 catalysts were recorded on a JEOL JDX-8P diffractometer using Cu$K\alpha$ radiation with a scan rate of 2° min^{-1}. BET surface area of samples were measured by nitrogen adsorption using a Micromeritics Accusorb Model 2100 instrument. Transmission electron microscopy (TEM) of Cu/CeO_2 was carried out using a JEOL JEM-200 CX transmission electron microscope to elucidate the microstructural features.

Cu/CeO_2 samples were also studied by X-ray photoelectron spectroscopy (XPS) using Al$K\alpha$ radiation in an ESCA-3 Mark II spectrometer (VG Scientific Limited, England) to examine the oxidation states of Ce and Cu before and after the catalytic reactions and to determine the surface segregations of Cu on CeO_2. Binding energies reported here are with reference to C(1s) at 285 eV.

Electron paramagnetic resonance (EPR) spectra of Cu/CeO_2 samples were recorded at 300 K using E-Line X-band Varian EPR spectrometer at a frequency of 9.5 GHz. The magnetic field was modulated at 100 kHz. The g values were calculated by comparison with a DPPH (diphenylpicrylhydrazyl) sample ($g = 2.0036$).

Temperature-Programmed Reaction (TPR)

Gas–solid reactions were carried out in a temperature-programmed reaction system equipped with a quadrupole mass spectrometer QXK300 (VG Scientific Limited, England) for product analysis (22). Typically, 0.2 g of the oxide catalyst was loaded in a quartz tube reactor 20 cm in length and 6 mm in diameter. The reactor was heated from 30 to 750°C at a rate of 15°C min^{-1} and the sample temperature was measured by a fine chromel–alumel thermocouple immersed in the catalyst. The quartz tube was evacuated to 10^{-6} Torr. The gases were passed over the catalyst at a flow rate of 20 μmol s^{-1} and it was varied from 10 to 40 μmol s^{-1}. Accordingly, the space velocity was in the range of 5×10^{-5} to 2×10^{-4} mol g^{-1} s^{-1}. Dynamic pressure of the gas mixture was varied from 200 to 500 mTorr in the reaction system and reactions were also carried out at dynamic pressure up to 1 Torr over 0.2 g of the catalyst. The gaseous products were leaked into an ultra high vacuum (UHV) system housing the quadrupole mass spectrometer at 10^{-9} Torr. A mixture of gases with known molar ratio was taken in 2-liter glass bulbs separately to carry out quantitative reactions. For 6 : 4 $NO + NH_3$ reaction partial pressures of NO and NH_3 in the bulb were 420 and 280 Torr, respectively. NO was obtained from Bhoruka Gases Limited, Bangalore, and CO was prepared in the laboratory. Purities of NO, NH_3, and CO were better than 99% as analyzed with a quadrupole mass spectrometer.

All the masses were scanned in every 10 s. Intensity of each mass as a function of temperature (thermogram) was generated at the end of the reaction. Intensity of any gas can be calculated by multiplying relative intensity from the mass spectrometric analysis with the ionization cross section of the particular gas (23). Relative intensities of H_2O ($m/e = 18$) and OH^+ ($m/e = 17$) were obtained by leaking H_2O vapor into the UHV system. Accordingly, when both NH_3 ($m/e = 17$) and H_2O were present in the gaseous products intensity of NH_3 was obtained by deducting the fraction due to OH^+ from the intensity of H_2O. Temperature-programmed desorption (TPD) was performed with all the catalysts up to 750°C and O_2 ($m/e = 32$), CO ($m/e = 28$) and CO_2 ($m/e = 44$) were not observed as desorption products. Further, TPR with only O_2 over these catalysts did not give CO_2 even up to 750°C, indicating that catalysts are free from any carbon impurity.

RESULTS

Structural Studies

X-ray diffraction patterns of CeO_2 and Cu doped CeO_2 are shown in Fig. 1. The diffraction lines are indexed to fluorite structure and the d values agree well with CeO_2. All the catalysts show broad XRD lines and the crystallite sizes calculated using the Debye–Scherrer method are in the range of 90–200 Å. Typical crystallite sizes of CeO_2, 5% Cu/CeO_2, and 10% Cu/CeO_2 are 150, 100, and 90 Å, respectively. The diffraction lines of Cu doped CeO_2 are broader than pure CeO_2. No change in the diffraction pattern in terms of line width is observed on heating these oxides at 300°C for 12 h. Increase in Cu content increases the line width with reference to CeO_2 (compare curves b and c with a). Since the lines are broad, impurity peaks, if any, due to

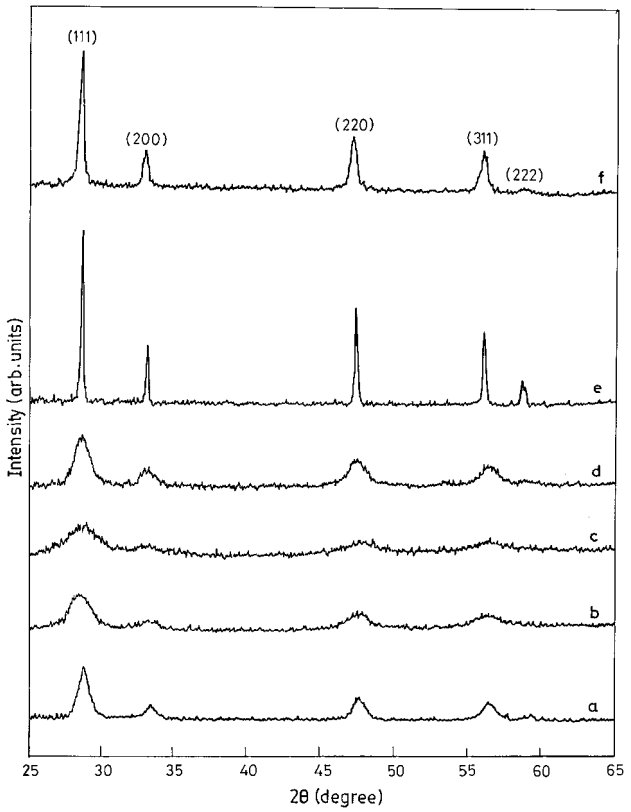

FIG. 1. XRD patterns of (a) CeO_2, (b) 5% Cu/CeO_2, (c) 10% Cu/CeO_2, (d) 5% Cu/CeO_2 after three cycles of $NO + NH_3$ reaction, (e) 5% Cu/CeO_2 sintered at 1000°C for 12 h, and (f) CeO_2 from the decomposition of ceric ammonium nitrate.

CuO could not be detected. Therefore, CeO_2, 5% Cu/CeO_2, and 10% Cu/CeO_2 samples were heated to 1000°C for 12 h to sinter the samples. No shift is observed in the diffraction lines of Cu/CeO_2 compared to pure CeO_2 either in the as-prepared or in the sintered samples. This suggests that Cu^{2+} may not be substituted for Ce^{4+} in CeO_2. Further, diffraction lines due to any of the oxides of Cu are not detected in the sintered sample (curve e). Increase in the line width of Cu/CeO_2 compared to pure CeO_2, absence of shift in the diffraction lines, and also the absence of CuO phase suggest that the Cu^{2+} ions are dispersed on the surface of CeO_2. There is a slight decrease in the line width of 5% Cu/CeO_2 after three cycles of catalytic reaction of NO with NH_3 from 30 to 450°C (curve d). Yet the crystallite sizes are still ~150 Å. The diffraction lines of CeO_2 prepared by the decomposition of ceric ammonium nitrate are much narrower than those of CeO_2 prepared by the solution combustion method (compare curves a and f). Diffraction patterns of Zr, Y, and Ca doped CeO_2 prepared by the combustion method were similar to those of pure CeO_2. The particle sizes of these materials were also in the range of 100–200 Å.

The surface areas of pure CeO_2 and Zr, Y, Ca, and Cu doped CeO_2 prepared here are in the range of 85–100 $m^2 g^{-1}$. Assuming the particles to be spherical and unagglomerated the particle sizes of CeO_2 and other oxides calculated from surface area are in the range of 100–200 Å (24). These values agree well with the XRD data. On the other hand, surface area and particle size of CeO_2 prepared from heating ceric ammonium nitrate are 14 $m^2 g^{-1}$ and 1050 Å, respectively.

Transmission electron microscopy of 5% Cu/CeO_2 shows that the crystallite sizes are less than 100 Å. This agrees well with the X-ray as well as surface area measurement. A typical TEM image is given in Fig. 2a. The ring-type diffraction pattern shown in Fig. 2b is indexed to polycrystalline CeO_2 in fluorite structure and no line corresponding to any of the oxides of Cu is detected. Also, no agglomerated CuO is detected in the TEM images. This again suggests that Cu^{2+} may be dispersed on the CeO_2 surface.

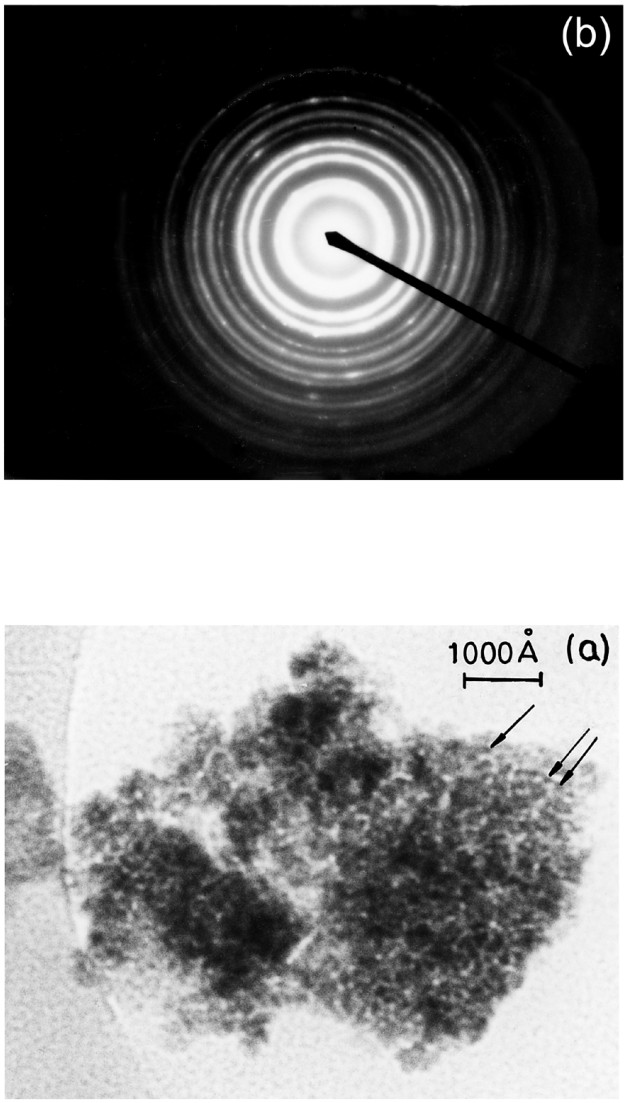

FIG. 2. (a) TEM of 5% Cu/CeO_2 and (b) electron diffraction pattern of 5% Cu/CeO_2.

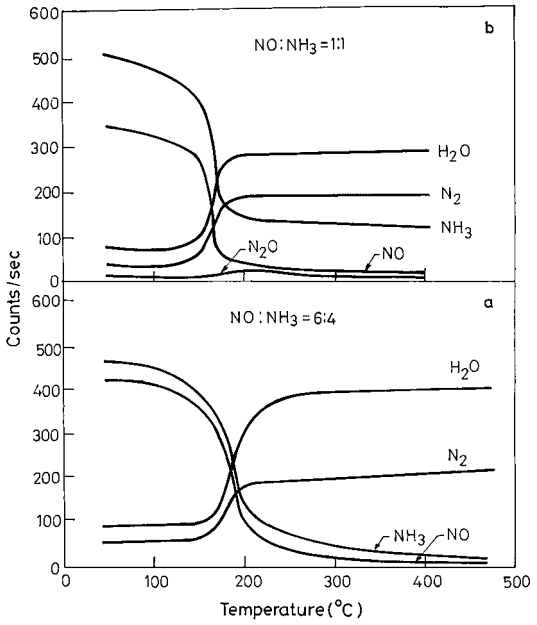

FIG. 3. TPR profiles of (a) $NO + NH_3$ (6 : 4) and (b) $NO + NH_3$ (1 : 1) over 5% Cu/CeO_2.

Temperature-Programmed Reaction

NO reduction by NH_3. NO reduction by NH_3 over 5% Cu/CeO_2 was carried out with $NO + NH_3$ in 6 : 4 and 1 : 1 molar ratios. Temperature profiles of the reactants and the products for the NO and NH_3 reaction over 5% Cu/CeO_2 catalyst are shown in Fig. 3. A sharp decrease in NO concentration is observed at 160°C and within 200°C over 88% conversion of NO is seen. Nearly 100% NO conversion occurs below 300°C (Fig. 3a). Also no NH_3 remains in the products above 300°C. However, when the NO concentration was low as in 1 : 1 NO and NH_3 mixture, mass peak at $m/e = 44$ is obtained in addition to N_2 and H_2O in the temperature range of 170 to 250°C (Fig. 3b). As there is no carbon impurity in the catalyst this $m/e = 44$ peak is attributed to N_2O. The intensity ratio of N_2 to N_2O is about 7 : 1. The formation of N_2O may be due to the partial reduction of NO. Above 300°C N_2O also decomposes. Although NO reduction is complete at about 300°C, excess NH_3 remains in the products indicating NH_3 slip (3). When the NO to NH_3 molar ratio was 6 : 4, both NO and NH_3 were completely utilized, giving the stoichiometric conversion

$$6NO + 4NH_3 \rightarrow 5N_2 + 6H_2O. \qquad [1]$$

When equimolar ratio of NO to NH_3 was taken, the reaction was as follows:

$$10NO + 10NH_3 \rightarrow 7N_2 + N_2O + 9H_2O + 4NH_3. \qquad [2]$$

These reactions suggest that oxygen from the catalyst surface may not be utilized in the reaction. Further, there is no decrease in the catalytic activity of 5% Cu/CeO_2 after three cycles of NO and NH_3 reaction. Also, at 300°C, isothermal reaction of NO reduction by NH_3 at 40 μmol s^{-1} flow rate shows complete conversion of NO even after 2 h.

The SCR of NO with NH_3 is based on the reaction

$$4NO + 4NH_3 + O_2 \rightarrow 4N_2 + 6H_2O. \qquad [3]$$

This process is well established and widely used for the abatement of NO from waste gases of stationary sources. So, NO and NH_3 gases were mixed in a 1 : 1 molar ratio and the reaction was carried out over 5% Cu/CeO_2 in the presence of 3–5 times excess O_2. The reaction profile is given in Fig. 4. NO reduction starts at 150°C and nearly complete NO reduction occurs below 300°C. NO reduction continues upto 350°C. At temperatures higher than 350°C NO reappears in the products. To study the role of NH_3 in the SCR of NO, NH_3 oxidation has been done over 5% Cu/CeO_2 in the presence of excess O_2. We find that NH_3 oxidation starts at 250°C giving N_2 and H_2O (Fig. 5a) and above 350°C, both N_2 and NO are the products having more NO concentration than N_2. Thus up to 350°C NH_3 oxidation over 5% Cu/CeO_2 follows the reaction

$$4NH_3 + 3O_2 \rightarrow 2N_2 + 6H_2O \qquad [4]$$

and, above 350°C, the reaction can be written as

$$4NH_3 + 4O_2 \rightarrow N_2 + 2NO + 6H_2O. \qquad [5]$$

From these studies, it is clear that SCR of NO with NH_3 over 5% Cu/CeO_2 in the presence of excess O_2 occurs in the temperature range of 150–350°C. Above this temperature NH_3 oxidizes to both N_2 of NO. On the other hand, when less O_2 is used for NH_3 oxidation over 5% Cu/CeO_2, only N_2 and H_2O are the products without NO even up to 650°C (Fig. 5b) following the reaction [4].

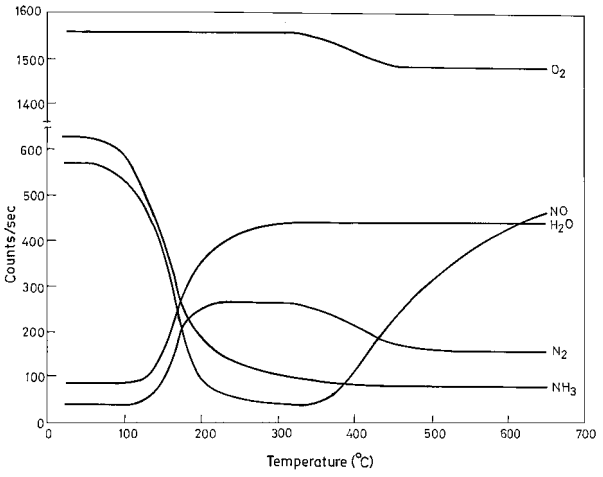

FIG. 4. TPR profile of $NO + NH_3$ reaction in the presence of excess O_2 over 5% Cu/CeO_2.

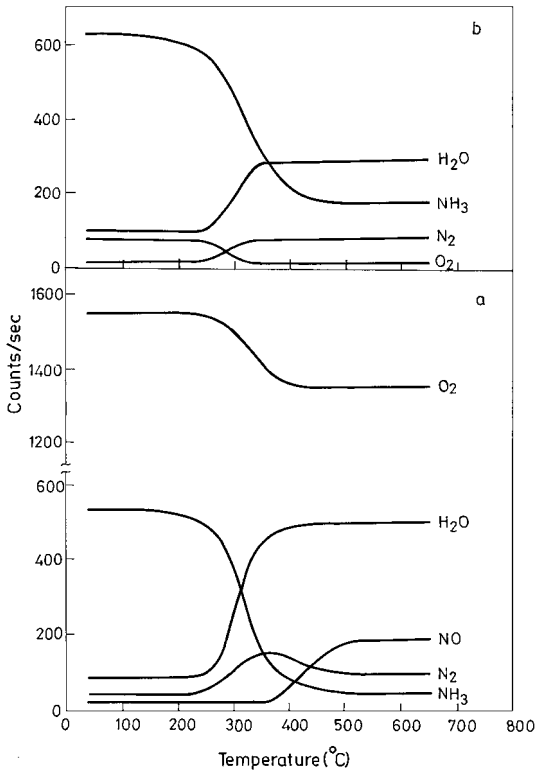

FIG. 5. TPR profiles of NH_3 oxidation in the presence of (a) excess O_2 and (b) less O_2.

NO reduction with NH_3 over CeO_2 and Zr, Y, and Ca doped CeO_2 were also studied. The rate of NO conversion as a function of temperature is given in Fig. 6 for $NO + NH_3$ reaction over all these catalysts where the NO to NH_3 molar ratio was 6 : 4. Rates (μmol m^{-2} s^{-1}) are calculated from the surface area of the catalysts and the flow rate (25). In the case of 5% Cu/CeO_2 conversion rates are much higher in

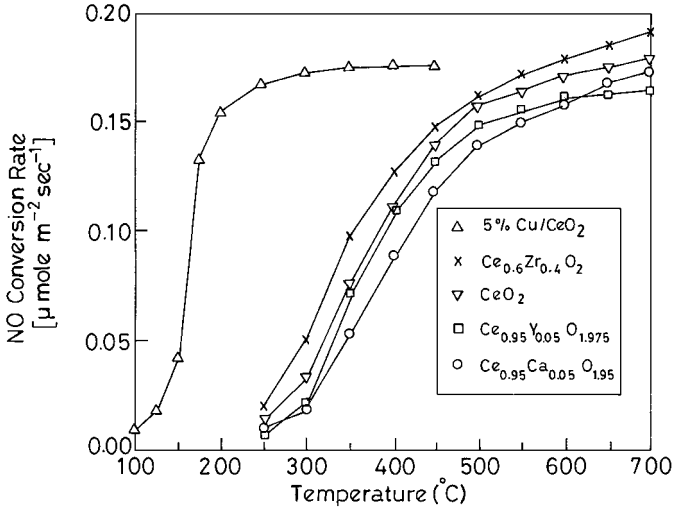

FIG. 6. Rate of NO conversion over ceria-based catalysts for $NO + NH_3$ (6 : 4) reactions as a function of temperature.

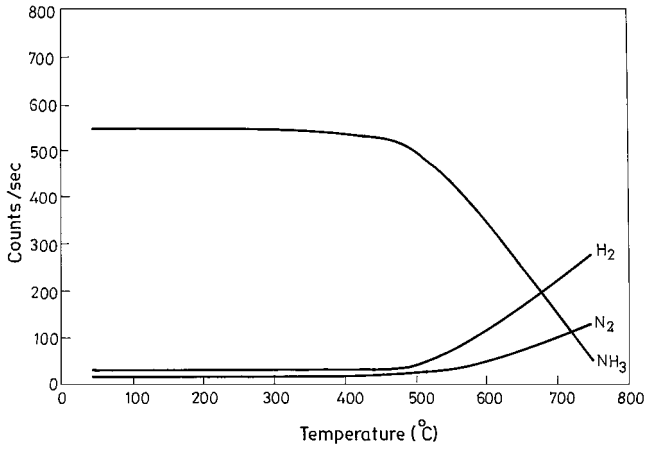

FIG. 7. TPR profile of NH_3 decomposition over 5% Cu/CeO_2.

the lower temperature region compared to other catalysts. Conversions are almost 100% as the curves in Fig. 6 line out.

To unequivocally prove the unique NO reduction over Cu/CeO_2, other catalytic reactions were also carried out: (i) Only NO gas was passed over 5% Cu/CeO_2 from 30 to 750°C and there was no reaction of NO with the catalyst. NO was not oxidized to NO_2. (ii) NH_3 over 5% Cu/CeO_2 gave N_2 and H_2 above 500°C (Fig. 7). (iii) NH_3 dissociated into N_2 and H_2 over pure CeO_2 above 600°C. (iv) Reactions were also carried out with 10% Cu/CeO_2. $NO + NH_3$ in 6 : 4 molar ratio over 10% Cu/CeO_2 showed a sharp decrease in NO at 190°C and complete reduction occurred below 350°C. An increase in the NO reduction temperature by about 30 to 40°C was observed with an increase in the Cu content. (v) NO reduction with NH_3 was also carried out with pure CuO and the products were N_2 and H_2O. NO conversion to N_2 starts at 250°C and nearly 100% conversion occurs at around 350°C. However, CuO is slowly reduced to Cu_2O as seen from the color and XRD studies.

NO reduction by CO. Equimolar mixture of NO and CO passed over 5% Cu/CeO_2 shows the formation of CO_2 at 160°C. Complete NO reduction occurs below 300°C. The reaction profile is shown in Fig. 8a. Mass peaks other than $m/e = 28$ and $m/e = 44$ were not observed in the gaseous products above 300°C. Total decrease of NO ($m/e = 30$) concentration indicates the total conversion of NO. Reaction with only NO over 5% Cu/CeO_2 did not give NO_2 ($m/e = 46$) and N_2O ($m/e = 44$). So, increase of $m/e = 44$ peak with simultaneous decrease of NO during the reaction must be due to increases in CO_2 ($m/e = 44$) from CO. Above 300°C when all NO is utilized, constant intensity of $m/e = 28$ and $m/e = 44$ peaks can be attributed to N_2 and CO_2. Therefore, we believe that the reaction may be written as

$$2NO + 2CO \rightarrow N_2 + 2CO_2. \quad [6]$$

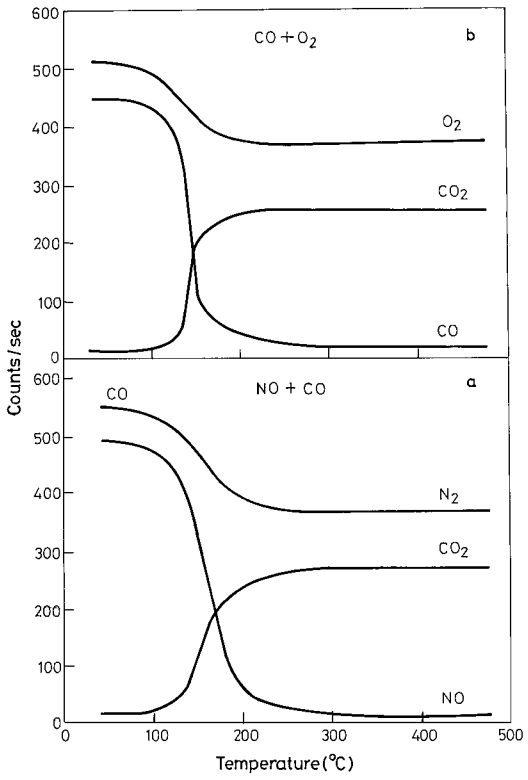

FIG. 8. TPR profiles of (a) NO + CO and (b) CO + O_2 reactions over 5% Cu/CeO_2.

When NO and CO were passed over pure CeO_2, NO reduction began at 300°C and complete utilization of NO and CO occured above 450°C. Thus, the catalytic behavior of 5% Cu/CeO_2 for CO oxidation by NO is similar to NO reduction by NH_3.

CO oxidation by O_2. CO oxidation over the same 5% Cu/CeO_2 catalyst is shown in Fig. 8b. The CO oxidation begins at about 160°C and complete oxidation is observed below 300°C. The reaction can be given by

$$2CO + O_2 \rightarrow 2CO_2. \qquad [7]$$

This result further supports reaction [6], indicating $m/e = 44$ due to CO_2. It is important to note that the study of CO oxidation by O_2 agrees well with similar work done by Flytzani-Stephanopoulos *et al.* over Cu/CeO_2 catalyst (17, 18).

NO reduction by hydrocarbon. Oxidation of hydrocarbon on 5% Cu/CeO_2 by NO is an important reaction that was also investigated here. First, cooking gas (INDANE) was used as a source of hydrocarbon that contains over 90% *n*-butane. In Fig. 9, mass spectra of NO and hydrocarbon at 60°C (curve a) and products N_2, H_2O, and CO_2 at 350°C (curve b) are presented. The mass peaks at $m/e = 29$, $m/e = 43$, and $m/e = 57$ correspond to *n*-butane fragments. At 350°C NO as well as hydrocarbon appear to be fully utilized as per the reaction

$$26NO + 2C_4H_{10} \rightarrow 13N_2 + 10H_2O + 8CO_2. \qquad [8]$$

Stoichiometric oxidation of CH_4 by NO was also carried out over 5% Cu/CeO_2 and N_2, H_2O, and CO_2 were the products. Complete conversion of NO occurs above 520°C.

Kinetics

The NO reduction by NH_3 over Cu^{2+}-impregnated zeolites follows first-order kinetics with respect to NO (11, 12). For a packed-bed tubular reactor the first-order rate constant (k) is given by (26–28)

$$k\ (\mathrm{cm^3\ g^{-1}\ s^{-1}}) = -\frac{F}{[\mathrm{NO}]W}\ln(1 - X), \qquad [9]$$

where k = rate constant, F = inlet molar flow rate of NO, [NO] = inlet molar concentration of NO, W = weight of the catalyst, and X = fractional NO conversion at a particular temperature. Keeping the flow rate constant (20 μmol s^{-1}) NO + NH_3 reaction was carried out with different amounts of catalyst ($W = 0.025$–0.10 g) over 5% Cu/CeO_2. A plot of $-\ln(1 - X)$ vs W/F gives a straight line passing through the origin, indicating that NO + NH_3 reaction follows first-order kinetics with respect to NO. Rate constants for NO reduction by NH_3 over 5% Cu/CeO_2 are in the range of 1.4×10^4 to 2.3×10^4 $\mathrm{cm^3\ g^{-1}\ s^{-1}}$ between 170 and 300°C.

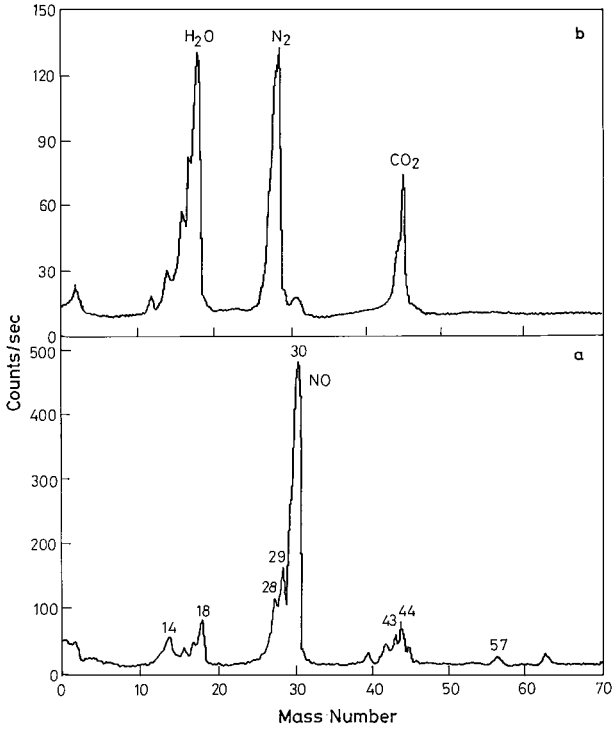

FIG. 9. Mass spectra of NO and hydrocarbon (*n*-butane) reaction (a) at 60°C and (b) at 350°C over 5% Cu/CeO_2.

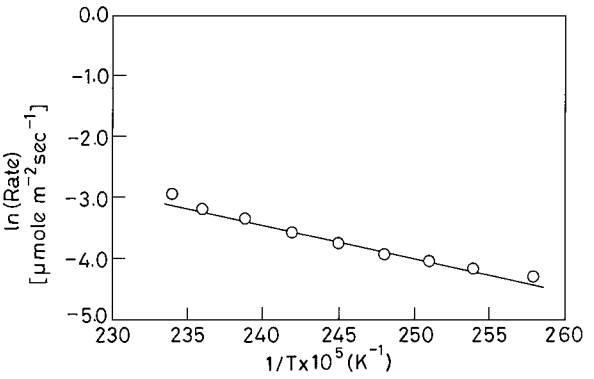

FIG. 10. Arrhenius plot for NO conversion rate of $NO + NH_3$ (6:4) reaction over 5% Cu/CeO_2.

The activation energy was obtained from an Arrhenius plot of ln(Rate) vs $1/T$ (Fig. 10) of $NO + NH_3$ (6:4) reaction. E_a value (44.7 kJ mol^{-1}) for NO reduction observed over 5% Cu/CeO_2 is lower than those reported for the same reaction over amorphous chromia (50 kJ mol^{-1}), Cu^{2+}-ZSM-5 (49 kJ mol^{-1}), V_2O_5 (49 kJ mol^{-1}), V_2O_5/TiO_2 (62 kJ mol^{-1}), and H-ZSM-5 (60.7 kJ mol^{-1}) (5, 11, 29–31). It is slightly higher than those for Cu^{2+}-MFI-ferrisilicate (37 kJ mol^{-1}), Fe-HMS (27.3 kJ mol^{-1}), and Fe-MCM-41 (16.8 kJ mol^{-1}) (12, 13). Activation energies of CO oxidation by NO (48.7 kJ mol^{-1}) over 5% Cu/CeO_2 are lower than those of CO oxidation by O_2 on $LaBa_2Cu_2CoO_{7+\delta}$ (57.2 kJ mol^{-1}) (32).

XPS Studies

X-ray photoelectron spectra of 10% Cu/CeO_2 in the Ce(3*d*) and Cu(2*p*) regions are given in Figs. 11a and 11b, respectively. The spectra of the oxide before and after the catalytic reaction ($6NO + 4NH_3$) were examined by XPS. The Ce(3*d*) spectrum with intense satellites marked in Fig. 11a identifies with Ce^{4+} in CeO_2 (33). No significant change is observed in the Ce(3*d*) spectrum after the reaction, indicating that there is no reduction of Ce^{4+} to Ce^{3+}. The XPS of Cu($2p_{3/2}$) in Fig. 11b shows that Cu is in +2 state as seen from the Cu^{2+}($2p_{3/2}$) binding energy as well as the satellite peaks. Here also no change in Cu(2*p*) spectrum is observed after the sample was subjected to NO reduction with NH_3, indicating that there is little reduction of Cu^{2+}. Almost no change is observed in the intensities of Ce(3*d*) and Cu(2*p*) spectra of the samples after the catalytic reaction. An estimation of surface concentration ratio of Cu/Ce from the Cu($2p_{3/2}$) and Ce($3d_{5/2}$) intensities is carried out as follows (34),

$$\frac{X_{Cu}}{X_{Ce}} = \frac{I[Cu(2p_{3/2})]}{I[Ce(3d_{5/2})]} \cdot \frac{\sigma_{Ce}\lambda_{Ce}D_E(Ce)}{\sigma_{Cu}\lambda_{Cu}D_E(Cu)}, \qquad [10]$$

where X_{Cu} and X_{Ce} are the surface concentrations, σ_{Cu} and σ_{Ce} are the photoionization cross sections, λ_{Cu} and λ_{Ce} are mean escape depths, and $D_E(Cu)$ and $D_E(Ce)$ are the geometric factors. Since both Cu(2*p*) and Ce(3*d*) signals are obtained in the same energy range (900–950 eV), D_E values are essentially the same for Cu(2*p*) and Ce(3*d*) core levels. Mean escape depths are taken from Penn (35) and photoionization cross section values are taken from Scofield (36). Intensities are obtained from the area under the peaks Cu($2p_{3/2}$) and Ce($3d_{5/2}$). The results calculated from Eq. [10] show that $X_{Cu}/X_{Ce} = 0.41$. Thus, the surface content of Cu is 41% against 10% by molar ratio taken in the preparation. A similar observation was made earlier on 1% Cu/CeO_2 (37). Therefore, XPS studies confirm the dispersion of Cu^{2+} on the surface of CeO_2 particles.

EPR Studies

EPR of 5% Cu/CeO_2 before and after catalytic reactions are presented in Fig. 12. The spectrum of as-prepared 5% Cu/CeO_2 (Fig. 12a) is characteristic of isolated Cu^{2+} ions in comparison with EPR of Cu/CeO_2 reported in the literature (37–40). The feature marked "K" in the figure has been attributed to a pair of two equivalent Cu^{2+} ions

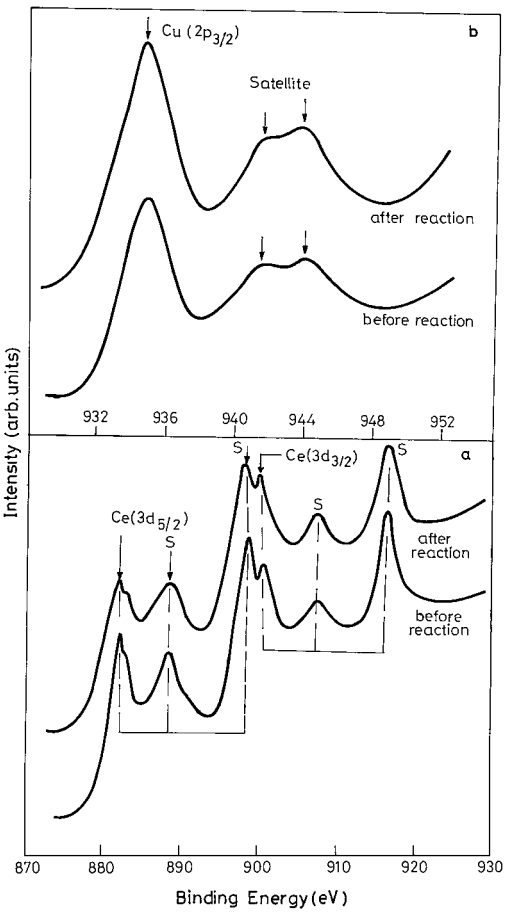

FIG. 11. XPS of (a) Ce(3*d*) and (b) Cu($2p_{3/2}$) regions of 10% Cu/CeO_2 before and after $NO + NH_3$ reactions.

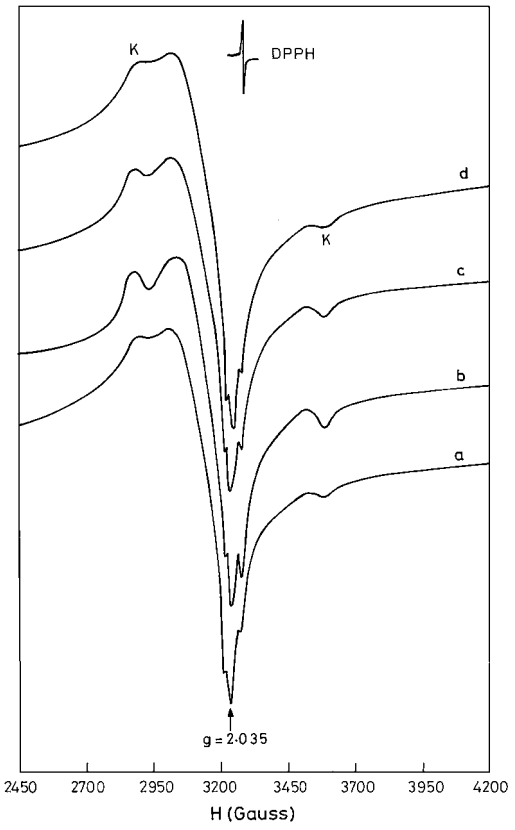

FIG. 12. EPR spectra of 5% Cu/CeO_2 (a) of freshly prepared dry sample, (b) after $NO + NH_3$ (6:4) reaction, (c) after $NO + NH_3$ (1:1) reaction, and (d) after $CO + O_2$ reaction.

separated by an oxygen with a distance of 3.4 Å which is smaller than the Ce–Ce distance (5.41 Å) in CeO_2. This shows that Cu^{2+} ions are not substituted for Ce^{4+} in CeO_2. There is a little change in the shape of EPR spectra after the catalytic reactions compared to one before the reaction (curves b, c, and d in Fig. 12).

DISCUSSIONS

SCR of NO by NH_3 primarily involves chemical reactions [1] and [3]. But reactions [4] and [5] are unwanted side reactions. It is well known that selectivity of SCR reaction couldn't be understood without investigating the role played by oxidation of NH_3. NH_3 oxidation over 5% Cu/CeO_2 starts around 250°C giving N_2 and H_2O and above 350°C N_2, NO, and H_2O are the products. So there is a competition between NO reduction by NH_3 and NH_3 oxidation by O_2 in the 250 to 350°C region during NO reduction by NH_3 in the presence of excess O_2. Since NO concentration comes down in this temperature region, NO reduction by NH_3 giving N_2 and H_2O predominates. On the other hand, above 350°C NH_3 oxidation predominates giving N_2, NO, and H_2O. Hence, NO concentration increases. Therefore Cu/CeO_2 catalyst is selectively active for NO reduction by NH_3 in the lower temperature region of 150 to 350°C. However, stoichiometric NO reduction reaction [1] occurs over 5% Cu/CeO_2 giving N_2 and H_2O as the products even up to 650°C.

NO reduction [1] over pure CeO_2 occurs above 600°C, whereas 100% conversion of NO has been observed over pure CuO at 350°C with the same reaction. Therefore, NO reduction occurring at a lower temperature (150°C) over 5% Cu/CeO_2 with Cu^{2+} ion on the surface indicates that Cu^{2+} ion is the active site of Cu/CeO_2 catalyst. The IR studies of NO adsorption on Cu^{2+}-based catalysts for NO conversion have been reported (41–43). Recently, Dandekar and Vannice (44) have studied the CO adsorption on supported Cu catalysts having different oxidation states by DRIFTS of chemisorbed CO. In our results the lowering of NO reduction temperature from 600 and 350°C over CeO_2 and CuO respectively, to 150°C over 5% Cu/CeO_2 suggests an additional interaction of Cu^{2+} ion with CeO_2 support. Understanding of the exact nature of this interaction needs further studies.

CONCLUSIONS

In conclusion, we have shown here a new method of catalyst preparation by the solution combustion process giving 100- to 200-Å crystallites of CeO_2 or Cu^{2+}-dispersed CeO_2 as characterized by XRD, TEM, XPS, and EPR techniques. Reactions of NO with NH_3, CO, and hydrocarbon with or without O_2 and NH_3 oxidation over Cu/CeO_2 have been examined by TPR. The salient findings are:

(a) The combustion process is simple, safe, and cost effective and takes 5 min to prepare one catalyst sample.

(b) Five percent Cu/CeO_2 shows selective catalytic reduction for NO by NH_3 in the low temperature window of 150–350°C and stoichiometric reduction of NO by NH_3 even up to 650°C.

(c) The activity of Cu/CeO_2 is superior to that of pure CeO_2 and Zr, Y, and Ca doped CeO_2 of similar particle sizes.

(d) NO is not oxidized to NO_2 over Cu/CeO_2.

(e) NH_3 oxidation in the presence of excess O_2 over 5% Cu/CeO_2 gives N_2 and H_2O below 350°C and N_2, NO, and H_2O above 350°C.

(f) Reduction of NO by NH_3 as well as CO and hydrocarbon occurs over 5% Cu/CeO_2 catalyst in the low temperature window of 150–350°C.

(g) Rate constants for NO reduction are in the range of 1.4×10^4 to 2.3×10^4 $cm^3\ g^{-1}\ s^{-1}$ between 170 and 300°C and the activation energy is 44.7 kJ mol^{-1} for $NO + NH_3$ (6:4) reaction.

ACKNOWLEDGMENTS

We thank Prathima Srinivasan for taking EPR spectra. Thanks are due to Dr. G. N. Subbanna for recording TEM. The authors P. Bera, S. T. Aruna,

and K. C. Patil are grateful to the Council of Scientific and Industrial Research (CSIR), New Delhi, for financial support.

REFERENCES

1. Argento, V. K., *Chem. Eng. Prog.* **84**, 50 (1988).
2. Janssen, F. J., *in* "Handbook of Heterogeneous Catalysis" (G. Ertl, H. Knözinger, and J. Weitkamp, Eds.), Vol. 4, p. 1633. VCH, Weinheim, 1997.
3. Radojevic, M., *Chem. Br.* **March**, 30 (1998).
4. Bosch, H., and Janssen, F. J., *Catal. Today* **2**, 369 (1988).
5. Curry-Hyde, E., and Baiker, A., *Ind. Eng. Chem. Res.* **29**, 1985 (1990).
6. Klimisch, R. L., and Taylor, K. C., *Ind. Eng. Chem. Prod. Res. Dev.* **14**, 26 (1975).
7. Bartholomew, C. H., *Ind. Eng. Chem. Prod. Res. Dev.* **14**, 29 (1975).
8. Bauerle, G. L., Wu, S. C., and Nobe, K., *Ind. Eng. Chem. Prod. Res. Dev.* **14**, 123 (1975).
9. Seiyama, T., Arakawa, T., Matsuda, T., Takita, Y., and Yamazoe, N., *J. Catal.* **48**, 1 (1977).
10. Brandin, J. G. M., Anderson, L. A. H., and Odenbrand, C. U. I., *Catal. Today* **4**, 187 (1989).
11. Komatsu, T., Nunokawa, M., Moon, I. S., Takahara, T., Namba, S., and Yashima, T., *J. Catal.* **148**, 427 (1994).
12. Komatsu, T., Ueda, T., and Yashima, T., *J. Chem. Soc. Faraday Trans.* **94**, 949 (1998).
13. Yang, R. T., Pinnavaia, T. J., Li, W., and Zhang, W., *J. Catal.* **172**, 488 (1997).
14. Taylor, K. C., *Catal. Rev. Sci. Eng.* **35**, 457 (1993).
15. Logan, A. D., and Shelef, M., *J. Mater. Res.* **9**, 468 (1994).
16. (a) Fornasiero, P., Monte, R. Di, Rao, G. R., Kašpar, J., Meriani, S., Trovarelli, A., and Graziani, M., *J. Catal.* **151**, 168 (1995); (b) Rao, G. R., Fornasiero, P., Monte, R. Di, Kašpar, J., Vlaic, G., Balducci, G., Meriani, S., Gubitosa, G., Cremona, A., and Graziani, M., *J. Catal.* **162**, 1 (1996); (c) Fornasiero, P., Balducci, G., Monte, R. Di, Kašpar, J., Sergo, V., Gubitosa, G., Ferrero, A., and Graziani, M., *J. Catal.* **164**, 173 (1996).
17. Liu, W., Sarofim, A. F., and Flytzani-Stephanopoulos, M., *Chem. Eng. Sci.* **49**, 4871 (1994).
18. Liu, W., and Flytzani-Stephanopoulos, M., *J. Catal.* **153**, 304 (1995).
19. Patil, K. C., Aruna, S. T., and Ekambaram, S., *Curr. Opin. Solid State Mater. Sci.* **2**, 158 (1997).
20. Suresh, K., and Patil, K. C., *in* "Perspectives in Solid State Chemistry" (K. J. Rao, Ed.), p. 376. Narosa, New Delhi, 1995.
21. Graw, G., *Anal. Chem. Acta.* **14**, 150 (1956).
22. Hegde, M. S., Ramesh, S., and Ramesh, G. S., *Proc. Indian Acad. Sci. Chem. Sci.* **104**, 591 (1992).
23. Kiser, R. W., "Introduction to Mass Spectrometry and Its Applications," p. 300. Prentice Hall, Englewood Cliffs, NJ, 1965.
24. Irani, R. R., and Callis, C. F., "Particle Size: Measurement, Interpretation and Applications," p. 125. Wiley, New York, 1963.
25. Burwell, R. L., Jr., *Pure Appl. Chem.* **46**, 71 (1976).
26. Thomas, J. M., and Thomas, W. J., "Introduction to the Principles of Heterogeneous Catalysis," p. 451. Academic Press, London, 1967.
27. Doraiswamy, L. K., and Tajbl, D. G., *Catal. Rev. Sci. Eng.* **10**, 177 (1974).
28. Kapteijn, F., and Moulijn, J. A., *in* "Handbook of Heterogeneous Catalysis" (G. Ertl, H. Knözinger, and J. Weitkamp, Eds.), Vol. 3, p. 1359, VCH, Weinheim, 1997.
29. Inomata, M., Miyamoto, A., and Murakami, Y., *J. Catal.* **62**, 140 (1980).
30. Baiker, A., Dollenmeier, P., Glinski, M., and Reller, A., *Appl. Catal.* **35**, 351 (1987).
31. Eng, J., and Bartholomew, C. H., *J. Catal.* **171**, 14 (1997).
32. Ramesh, S., and Hegde, M. S., *J. Phys. Chem.* **100**, 8443 (1996).
33. Sarma, D. D., Kamath, P. V., and Rao, C. N. R., *Chem. Phys.* **73**, 71 (1983).
34. Powell, C. J., and Larson, P. E., *Appl. Surf. Sci.* **1**, 186 (1978).
35. Penn, D. R., *J. Electron Spectrosc. Relat. Phenom.* **9**, 29 (1976).
36. Scofield, J. H., *J. Electron Spectrosc. Relat. Phenom.* **8**, 129 (1976).
37. Kaïs, A. A., Bennani, A., Aïssi, C. F., Wrobel, G., and Guelton, M., *J. Chem. Soc. Faraday Trans.* **88**, 1321 (1992).
38. Clementz, D. M., Pinnavaia, T. J., and Mortland, M. M., *J. Phys. Chem.* **77**, 196 (1973).
39. Kaïs, A. A., Bennani, A., Aïssi, C. F., Wrobel, G., Guelton, M., and Vedrine, J. C., *J. Chem. Soc. Faraday Trans.* **88**, 615 (1992).
40. Soria, J., Conesa, J. C., Martínez-Arias, A., and Coronado, J. M., *Solid State Ionics* **63–65**, 755 (1993).
41. London, J. W., and Bell, A. T., *J. Catal.* **31**, 32 (1973).
42. Giamello, E., Murphy, D., Magnacca, G., Morterra, C., Shioya, Y., Nomura, T., and Anpo, M., *J. Catal.* **136**, 510 (1992).
43. Centi, G., Nigro, C., Perathoner, S., and Stella, G., *Catal. Today* **17**, 159 (1993).
44. Dandekar, A., and Vannice, M. A., *J. Catal.* **178**, 621 (1998).